2019년 8월
교육학석사(기계·금속)학위논문

Microfluidics for Rheological Study

조선대학교 교육대학원

기계·금속교육전공

정 지 운

Microfluidics for Rheological Study

혈유변학 연구를 위한 미세유체역학

2019년 8월

조선대학교 교육대학원

기계·금속교육전공

정 지 운

Microfluidics for Rheological Study

지도교수 강 양 준

이 논문을 교육학석사(기계·금속)학위 청구논문으로 제출함.

2019년 4월

조선대학교 교육대학원

기계·금속교육전공

정 지 운

정지운의 교육학 석사학위 논문을 인준함.

심사위원장 조선대학교 교수 장 완 식 인

심사위원 조선대학교 교수 박 정 수 인

심사위원 조선대학교 교수 강 양 준 인

2019년 6월

조선대학교 교육대학원

Contents

List of figures

국문 초록

혈유변학 연구를 위한 미세유체역학

정 지 운
지도교수: 강 양 준
기계·금속교육전공
조선대학교 교육대학원

심혈관질환(CVDs)은 선진국의 주요 사망원인이며 미국 전체 사망자의 31.3%~32.8% 를 차지한다. 심혈관질환과 혈액 생물 물리학적 성질(즉, 적혈구 침강속도 [ESR], 헤마토크릿 및 점도) 사이의 밀접한 관계가 보고되었기 때문에 혈액 생물 물리학적 특성이 심혈관질환을 모니터하기 위해 주의를 끌고 있다. 심혈관질환은 혈장 단백질의 농도를 급격히 증가시킨다. 그러면 ESR이 크게 향상된다. 따라서 혈액의 생물리학적 특성 (즉, RBC 변형성 및 ESR)에 대한 혈장 및 적혈구의 개별 효과를 조사할 필요가 있다. 즉, RBC 및 혈장의 변화는 RBC 변형성과 ESR을 동시에 측정하여 효과적으로 관찰할 수 있다. 본 연구에서는 ACS에서 부유 혈액의 부피를 정량화함으로써 ESR 및 RBC 변형성을 순차적으로 측정하는 간단한 방법을 보여준다. 제안된 방법을 입증하기 위해 마이크로유체장치는 다중 마이크로 기둥 채널, 입구 및 출구로 구성된다. ACS는 일회용 주사기와 고정품으로 구성된다. ACS는 부분적으로 공기(~0.4mL)와 혈액(~0.6mL)으로 넣고 스토퍼로 콘센트를 닫음으로써 ACS의 바늘이 입구에 단단히 고정된다. 조명기를 사용하여 공기 압축의 볼륨이 V_{comp}의 특정 값으로 조정되고 스마트폰 카메라를 사용하여 스냅 샷 이미지를 순차적으로 캡처하여 ACS 내부의 정지된 혈액의 양(즉, V_{susp})을 관찰한다. 콘센트가 닫히면 V_{susp}가 V_{susp}=0.2mL가 될 때까지 V_{susp}의 변화가 얻어진다. ESR 지수 (즉, V_{ESR})는 V_{susp}의 시간 변화를 정량화함으로써 얻어진다. 한편, 콘센트를 개방 시, V_{susp}가 V_{susp}=0으로 감소될 때까지 V_{susp}의 변화가 얻어지고 시간에 따른

V_{susp}의 변화를 분석하여 RBC deformability index (V_{DI})를 얻었다. 실험 시연에서 첫째, V_{DI}에 대한 기둥 채널 길이 (L)의 효과는 L=50, 150 및 250μm를 변화시켜 정량화되었다. L=150μm 이상에서는 V_{DI}가 유의한 차이를 보이지 않았고 이에 따라서 기둥 채널의 길이는 모든 실험을 통해 L=150μm로 고정하게 되었다.

둘째, V_{ESR} 및 V_{DI}에 대한 공기압축의 효과는 공기압축체적 (V_{comp}) (V_{comp}=0.2, 0.3 및 0.4mL)을 변화시킴으로써 정량화되었다. V_{comp}는 VDI의 변화에 크게 기여했다. 그러나 ESR 지수를 변경시키지는 않았다. 따라서 공기압축의 부피 (V_{comp})는 모든 실험을 통해 V_{comp}=0.4 mL로 고정되었다. 세 번째로, V_{ESR}과 V_{DI}의 적혈구 용적률의 영향은 적혈구 용적률 (Hct) (Hct=20%, 30%, 40%, 50%)을 변화시켜 평가 하였다. 헤마토크릿이 높을수록 ESR 및 RBC 변형 측정시간이 많이 증가하였다. 넷째, 제안된 방법은 Dextran을 포함한 혈액에 대한 V_{ESR}과 V_{DI}를 측정하기 위해 사용된다. Dextran 용액은 ESR의 경과 시간을 많이 감소시키는데 기여한다. 그러나 그것은 RBC 변형성의 경과 시간에는 영향을 미치지 않았다. 마침내 제안된 방법은 이종 혈액을 검출하는데 사용된다. 2개의 지표 (즉, V_{ESR} 및 V_{DI})는 ϕ=10% 보다 상당히 가변적이다. 그 결과로부터 제안된 방법은 적어도 10%의 경화된 혈액으로 이종 혈액을 검출할 수 있다는 결론을 이끌어 낸다. 또한 ESR 및 RBC 변형성을 효과적으로 정량화하기 위해 두 개의 지표 (즉, V_{ESR} 및 V_{DI})가 사용된다.

키워드 : RBC 변형성; 적혈구 침강 속도(ESR); 미세유체시스템;
스마트폰 카메라; 공기 압축주사기(ACS)

I. Introduction

Cardiovascular diseases (CVDs) are the leading causes of death in advances countries, and account for 31.3% ~ 32.8% of all deaths in United States[1]. The CVDs, including coronary heart diseases, stroke, atherosclerosis, myocardial infarction, occurs suddenly without any symptoms or warmings. Because vascular blockage or blood clotting interrupts blood flows in microcirculation, the CVDs contribute to serious complications or unexpected deaths[2]. However, biochemical properties of blood, including biomarker, cholesterol, and glucose, still include clinical issues on early detection of CVDs[3]. Since the strong relationship between CVDs and blood biophysical properties (i.e., erythrocyte sedimentation rate [ESR], hematocrit, and viscosity) was reported, blood biophysical properties are paid attention to monitor CVDs[4,5].

Microcirculation is the circulation of blood through the smallest blood vessels, including capillary networks, arterioles, and venules[6]. It plays a vital role in regulating blood flows in organs, and exchanging substances between blood and peripheral tissues. Because microcirculatory disorders lead to mortality, it is required to understand how blood properties and blood flows have an influence on exchange in the microcirculation[6].

Blood is a concentrated suspension of formed elements (red blood cells [RBCs], white blood cells, and platelets) and blood plasma. Under physiological condition, RBCs occupy 40%-50% of blood volume (i.e., hematocrit [Hct]=40%-50%). White blood cells and platelets occupy ~1/600

of blood volume, and ~1/800 of blood volume, respectively[6]. Due to high abundance of RBCs in blood, biophysical properties of blood are dominantly determined by those of the RBCs[7]. Thus, blood biophysical researches focus on RBCs-related properties, including hematocrit, blood viscoelasticity, RBC deformability, and RBC aggregation[8]. Due to its high deformability under blood flow, individual RBC has ability to easily pass through micro-size capillary vessels. Here, RBC deformability is determined significantly by several factors, including membrane cytoskeleton, cytoplasmic viscosity, and surface area/volume ratio[9]. Hematologic disorders, including malaria-infected RBCs, sepsis, and diabetes, cause to decrease RBC deformability largely[10]. RBC deformability[9,11-26] is considered as contributing factor to blood viscosity[14,27-29], and RBCs aggregation[30-37]. On the other hand, the ESR is observed with naked eye by quantifying interface between cells and plasma in the Westergren sedimentation tube (inner diameter=2.5mm, length=200mm, and blood volume=5mL) in 1h[38]. Because it is simple and inexpensive test, the ESR still provides useful index of non-specific disease activity in clinical settings[38]. The kinetics of ESR consists of three different phases, and follows an S-shaped curve with an elapse of time[39]. Because blood flow is extremely low in the Westergren sedimentation tube, RBC aggregates and forms rouleaux. Thus, RBC aggregation accelerates ESR over time. The ESR is varied by several factors, including hematocrit, plasma protein level, and surface property of RBCs. Inflammatory diseases cause to increase the concentration of acute-phase plasma proteins. The ESR is then enhanced

significantly[37]. Thus, it is required to investigate the individual effect of plasma and RBCs on the biophysical properties of blood (i.e., RBC deformability and ESR). In other words, change in RBCs and plasma can be effectively monitored by measuring RBC deformability and ESR simultaneously.

Conventional method for measuring ESR and RBC deformability includes several disadvantages. The conventional Westergren ESR method shows several drawbacks, including long time measurement (~1h), bulk-sized instrument, and repetitive cleaning procedure. The conventional RBC deformability methods, such as a membrane filter[40] and a laser diffractometry[41] have several disadvantages. Large variations in the pore size of membrane filter cause to deteriorate repetitive performance. Because the laser diffractometry measure averaged deformability of RBCs by quantifying diffraction image of blood flow, it is not effective to discriminate minor difference in subpopulations of RBCs. The microfluidic platform can provide several advantages, including small volume consumption, disposability, and consistent performance.

Several methods such as electric impedance, microscopic image, and photometric method have been suggested to quantify ESR. First, electric impedances (i.e., resistance, capacitance, and conductivity) have been employed to monitor ESR inside plastic tube[42,43] or PDMS chamber[44]. Second, while turning upside down driving syringe in gravitational direction[45], blood is supplied from the top layer of the syringe into microfluidic device. The ESR is then monitored by quantifying image

intensity of continuous blood flow in microfluidic channel. To simultaneously measure RBC aggregation and ESR in a twin channel, blood is supplied from button layer of the upright driving syringe into a microfluidic device by turning off syringe pump periodically. The ESR and RBC aggregation are measured periodically by quantifying cell-to-liquid interface in counter-fluid channel and image intensity of blood flow in blood channel, respectively[46]. To remove a highly expensive and bulky syringe pump, a disposable air-suction pump and a pinch valve are suggested to delivery and stop blood from a conical pipette tip to a microfluidic device[47]. To measure multiple values of ESR in single experiment, blood is supplied from the conical pipette tip into parallel microfluidic channels (i.e., n=4) by turning on and off syringe pump periodically[33]. Four values of ESR are obtained periodically by analyzing image intensity of blood. While setting microfluidic channel vertically in gravitational.

direction, ESR is then obtained by measuring setting velocity of RBCs in microfluidic channel[48]. Third, after disposable cartridge is filled with bloods, RBCs aggregate or disaggregates by turning on or off a solenoid pinch valve. An infrared emitting diode is used to illuminate bloods filled in the cartridge. The transmitted light through the cartridge is measured by using a photodetector. ESR is then obtained by quantifying the temporal variations of transmitted signals[49].

Under microfluidic platform, several methods such as cell blockage, cell aspiration, cell transit, and electric impedance are suggested to measure deformability of individual RBCs. First, clogging in single constriction

channel[50], capillary network[51], and gradual filter with variable pores is employed to quantify deformability of malaria-infected RBCs[50], hardened RBCs[51,52], and circulating leukocytes (i.e., THP-1, and ARDS)[52]. Minimum cylinder diameter of cells trapped in the parallel taper channels is calculated to discriminate difference in deformability of normal RBCs and malaria-infected RBCs[13]. Second, to detect lung tumor or malaria-infected RBCs, Young's modulus or cortical tension is quantified by suctioning single cell into single constriction[53] or multiple funnel channels[54], Third, by supplying single cells into capillary networks[55] or parallel micro constrictions[56], transit time of each cell is employed to detect sepsis or leukostasis. While delivering individual RBCs into triangular-shaped pillar channels, RBC velocity is quantified to detect malaria-infected RBCs. Single cell-based deformability give high sensitivity, throughput remains as critical issue. To improve throughput, blood (Hct=50%) is supplied into multiple pillar channel by using syringe pump. Deformability of RBCs is quantified by analyzing averaged blood velocity obtained from the micro-particle image velocimetry (PIV) technique. Furthermore, a disposable air-compressed pump is employed to supply bloods into multiple pillar channels. Without operating syringe pump and conducting micro-PIV technique, RBCs deformability is obtained by analyzing cell-to-liquid interface as pressure sensor. At last, while supplying individual RBCs into constriction channel, RBC deformability is obtained by analyzing variations of electric impedance (i.e., magnitude, and phase) over time[57,58]. Most previous methods did not have the ability to measure ESR and RBCs

deformability simultaneously. In addition, bulk-sized facilities including syringe pump, microscope, and high-speed camera, are required essentially to delivery blood or capture microscopic images of blood flows. Due to the facilities, most methods are demonstrated appropriately in laboratory environment, rather than in resource-limited environment. To resolve these issues, a new method should be devised for blood delivery, and image acquisition. In addition, ESR and RBC aggregation should be measured to investigate the individual effect of RBCs and plasma in a biomechanical point of view.

In this study, a simple method for sequential measurement of ESR and RBC deformability is proposed by quantifying the volume of suspended blood in an air-compressed syringe(ACS). To demonstrate the proposed method, a microfluidic device is composed of multiple micropillar channel, inlet, and outlet. The ACS is composed of a disposable syringe and a fixture. The disposable syringe is partially filled with air (~0.4mL), and blood (~0.6mL). By closing the outlet with a stopper, the disposable syringe is tightly fitted into the inlet. To increase pressure inside the syringe, cavity volume decreases to 0.4mL by moving plunger forward, and fastening it with a fixture component. Using smartphone camera, snapshot images are sequentially captured to monitor the volume of suspended blood inside the syringe (i.e., V_{susp}). ESR index (V_{ESR}) is obtained by quantifying the variations of V_{susp} over time. After the Vsusp is decreased to a specific value of V_{susp}=0.2mL, the stopper is removed immediately. Due to pressure developed inside the syringe, blood flows in the parallel micropillar

channels continuously. The Vsusp is varied by deformability of RBCs. Thus, RBC deformability index (V_{DI}) is similarly obtained by analyzing variations of Vsusp over time.

When compared with the previous methods, the proposed methods give distinctive two advantages. First, the proposed methods does not require bulky and expensive facilities, including, microscope, high-speed camera, and syringe pump. Due to the merit, the method promises high potentials for resource-limited settings. Second, the method has the ability to measure ESR and RBC deformability by analyzing the volume of suspended blood inside a syringe simultaneously.

As a performance demonstration, first, the changes in two indices (i.e., V_{ESR} and V_{DI}) are quantified by varying several factors (i.e. pillar-channel length, air-compression volume, and blood hematocrit [Hct]). Second, to stimulate ESR of blood, blood samples are prepared by adding normal RBCs into various concentrations of dextran solution. Using the proposed method, the variations of V_{ESR} and V_{DI} are obtained with respect to concentrations of dextran solution. At last, the proposed method is employed to detect variations of V_{ESR} and V_{DI} with respect to heterogeneous bloods. Here, heterogeneous bloods are prepared by mixing normal bloods with hardened bloods partially.

II. Materials and methods

A. Blood sample preparation

In accordance with the ethics committee of Chosun University Hospital (CUH), all the experiments were performed by ensuring that the procedures were appropriate and humane. Concentrated RBCs and fresh freeze plasma (FFP) were purchased from the Gwangju-Chonnam blood bank (Gwangju, Korea), and were stored at 4°C and -20°C, respectively. Blood was prepared by adding concentrated RBCs into PBS (Phosphate-Buffered Saline) solution (1×, pH 7.4, Gibco, Life Technologies, Korea). Using a centrifugal separator, pure RBCs were collected by removing a buffy layer and PBS. The washing procedure was conducted twice for all blood samples. After the FFP thawed in room temperature, a syringe filter of mesh size=5μm (Minisart, Sartorius, Germany) was applied to remove debris included in plasma. Several suspended bloods were prepared by adding normal RBCs into base solutions (i.e., PBS [Phosphate-buffered saline], and autologous plasma).

First, to evaluate the effect of the haematocrit on ESR and RBC deformability, hematocrit (Hct) of blood was adjusted to Hct=20%, 30%, 40%, and 50% by adding normal RBCs into a specific concentration of dextran solution (15mg/mL). Second, to stimulate ESR of blood, five different concentrations of dextran solution ($C_{dextran}$=5, 10, 15, 20, and 25mg/mL) were diluted by mixing dextran (*Leuconostoc* spp., MW=450-650 kDa, Sigma-Aldrich, USA) with PBS. Subsequently, bloods (Hct=30%) were prepared by adding normal RBCs to specific concentrations of dextran solution. As control, normal blood (Hct=30%) was prepared by adding

normal RBCs into plasma. Third, to vary deformability of RBCs, four different concentrations of glutaraldehyde (GA) solution (C_{GA}=2, 4, 6, and 8μL/mL) were diluted by mixing GA solution (Grade II, 25% in H_20, Sigma-Aldrich, U.S.A.) into PBS. Hardened RBCs were prepared by exposing normal RBCs into each concentration of GA solution for 10min. Hardened bloods (Hct=30%) were then prepared by adding hardened RBCs into PBS (i.e., V_{GA}). To reduce experimental time of ESR, normal blood (Hct=30%) was prepared by adding normal RBCs into the specific concentration of dextran solution (15mg/mL) (i.e., V_{dex}). The heterogeneous bloods were prepared by mixing hardened blood with normal blood partially. A mixing ratio (ϕ) was defined as $\phi = \frac{V_{GA}}{V_{GA} + V_{dex}}$. To quantify the effect of ϕ on the V_{ESR} and V_{DI}, the ϕ was prepared as ϕ=0, 5%, and 10%. Here, ϕ =0 indicated that blood did not include hardened blood.

B. Fabrication of a microfluidic device and experimental procedure

A microfluidic device for sequentially measuring ESR and RBC deformability consisted of inlet, outlet, and micropillar channel as shown in **Fig. 1-1**. The straight channel (width=250μm) was connected to the micropillar channels from inlet and outlet. As shown in **Fig. 1-1**, the micropillar channel composed of multiple narrow-sized channels (N=43, gap=4 μm, and channel length [L]=50, 150, and 250μm). The channel depth of the microfluidic device was fixed at 10μm. A conventional micro-electromechanical- system fabrication technique such as photolithography, and deep RIE (reactive iron etching) was employed to fabricate a

silicon-master mold. Polydimethyl siloxane (PDMS) (Sylgard 184, Dow Corning, Midland, MI, USA) was mixed with a curing agent at a ratio of 10:1. The PDMS mixture was poured on the mold. Air bubbles in PDMS were removed completely by operating a vacuum pump for 1 h. After curing the PDMS mixture in a convective oven at 70°C for 1h, a PDMS block was peeled off from the mold, and was cut with a razor blade. Inlet and outlet were punched with a biopsy punch (outer diameter=1.0mm). After surfaces of the PDMS block and a slide glass were treated with oxygen plasma system (CUTE-MPR, Femto Science Co., and South Korea), a microfluidic device was finally prepared by bonding the PDMS block on the slide glass.

As shown in **Fig. 1-1**, to remove bulk-size syringe pump, an air-compressed syringe (ACS) partially filled with air and blood was prepared by assembling a disposable syringe (~1mL) and a fixture. As shown in **Fig. S1 (Supplementary Materials)**, the dimensions of the fixture were determined to fix the plunger in the syringe securely. The fixture was then fabricated by using a 3D printer (Ultimaker 2+, Ultimaker B.V., and Netherlands). Due to air compression inside the syringe, blood inside the syringe was supplied into the microfluidic device. Here, to stop or run blood flows in the microfluidic channel, a stopper was tightly fitted into the outlet or removed from the outlet. As shown in **Fig. S2 (Supplementary Materials)**, the stopper was fabricated by using the 3D printer.

To remove air bubble in the channels and avoid non-specific binding of plasma proteins to the inner surface of the channels, the channel was filled with BSA (Bovine Serum Albumin) solution (C_{BSA}=2mg/mL) through the outlet with a disposable syringe. After an elapse of 5 min, after a stopper was tightly fitted into the outlet, the needle of the ACS was inserted into

the inlet. After the volume of suspended blood inside the ACS (i.e., V_{susp}) reduced to a specific value of V_{susp}=0.2mL, blood was supplied into the microfluidic channel from the ACS.

As shown in **Fig. 1-1**, a smartphone camera (Galaxy A5, Samsung, Korea) was employed to capture the snapshot images on the ACS over time. Snapshot images were sequentially captured at an interval of 5s, for a specific duration of time. Variations of V_{susp} was quantified by inspecting interfacial location between RBC-depleted layer and RBC-rich layer, for individual image captured at a specific time. All experiments were conducted at a room temperature of 25°C.

Figure 1-1. A proposed method for simultaneous measurement of ESR and RBC deformability. A schematic diagram of the proposed method, including air-compressed syringe (ACS), a microfluidic device, and a smartphone camera. The ACS was inserted into inlet port of the microfluidic device.

- A microfluidic device was composed of one inlet, one outlet, and micro-pillar channel. Blood flow was stopped by inserting into the outlet with a stopper. After an elapse of certain time, blood was flowed continuously by removing the stopper.
- Multiple micropillar channels (N=43, Gap=4μm, and depth=10μm)
- The ACS was composed of a disposable syringe (~1mL), and a fixture.
- A smartphone camera was employed to capture interfacial location between cell-free layer and cell-rich layer inside the syringe at an interval of 5s.

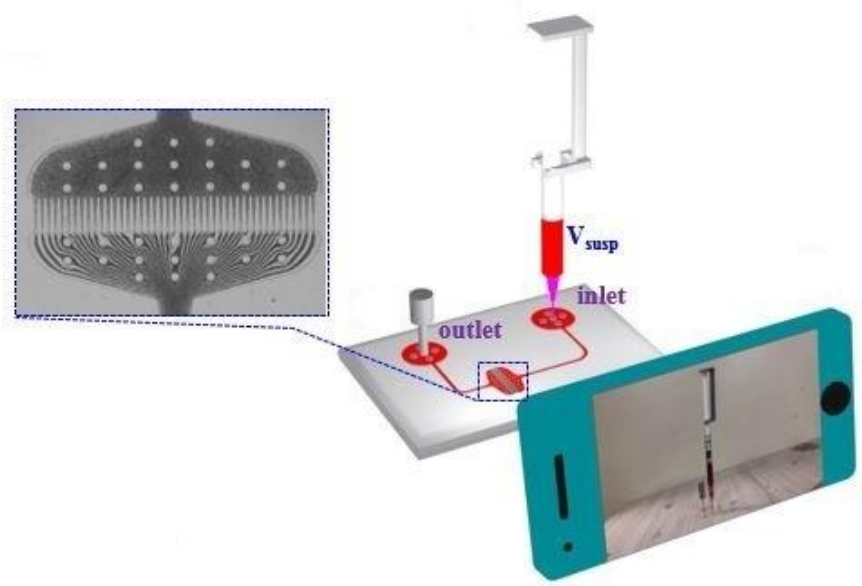

Figure 1-1 Simultaneous measurement of ESR and RBC

C. Operation of the ACS

As shown in **Fig. 1-2**, the ACS was suggested for delivering bloods into a microfluidic device. The operation of the ACS was divided into five stages. First, air (~0.4mL) was secured by moving plunger backward. Second, blood (~0.6mL) was suctioned by moving plunger backward. Third, to close the outlet of the microfluidic device, the stopper was tightly fitted into the outlet. Fourth, by securing the end of the plunger and syringe with the fixture, air cavity inside the syringe was adjusted to a specific value of V_{comp}=0.4mL. At last, using a stopwatch, the variations of V_{susp} in the syringe were monitored over time. Until V_{susp} decreased to 0.2mL, the outlet remained closed. Here, to easily monitor the variations of V_{susp}, snapshot images with an ACS and a stopwatch were captured sequentially

by using a smartphone camera. On the other hand, by removing the stopper from the outlet, snapshot images were captured sequentially by using the smartphone.

Figure 1-2 The operation of the ACS

D. Quantification of ESR and RBC deformability

As a preliminary study, suspended blood (Hct=30%) was prepared by adding normal RBCs to a specific concentration of the dextran solution (i.e., C_{dex}=15mg/mL). The ACS was filled with the suspended blood. **Figure 1-3** showed snapshot images captured at a specific time(t) at the close of outlet (t=198, 347, 402, 455, 533, and 582s). With an elapse of time, ESR caused

to decrease V_{susp}. On the other hand, by removing the stopper from the outlet, blood was supplied into the microfluidic device from the ACS. **Figure 1-3** illustrated snapshot images captured at a specific time(t) at the open of outlet (t=589, 615, 662, 749, 962, and 1145s). The V_{susp} was decreased gradually over time. As shown in **Fig. 1-4**, by inspecting interfacial location inside the ACS, variations of V_{susp} were obtained over time. To quantify ESR and RBC deformability, two indices were suggested as V_{ESR} for ESR and V_{DI} for RBC deformability, respectively.

First, at the close of outlet, the variations of V_{susp} were monitored continuously until the V_{susp} decreased to 0.2mL. ESR index (i.e., V_{ESR}) was quantified by integrating the variation of V_{susp} for a specific duration of $t=t_1$ (i.e., $V_{ESR} = \int_0^{t1} V_{susp} dt$). Here, $t=t_1$ indicated the specific time when the V_{susp} equaled to 0.2mL. Second, after removing the stopper, the variations of V_{susp} were monitored continuously until the V_{susp} decreased to zero value. Here, $t=t_2$ indicated the specific time when the V_{susp} equaled to zero. Based on similar approach of the ESR index, RBC deformability index (i.e., V_{DI}) was quantified by integrating the variation of V_{susp} from $t=t_1$ to $t=t_2$ (i.e., $V_{DI} = \int_{t1}^{t2} V_{susp} dt$).

In other words, by fitting the stopper into the outlet, ESR was evaluated by inspecting interfacial location in the ACS. After then, by removing the stopper from the outlet, RBC deformability was quantified by monitoring interface location in the ACS.

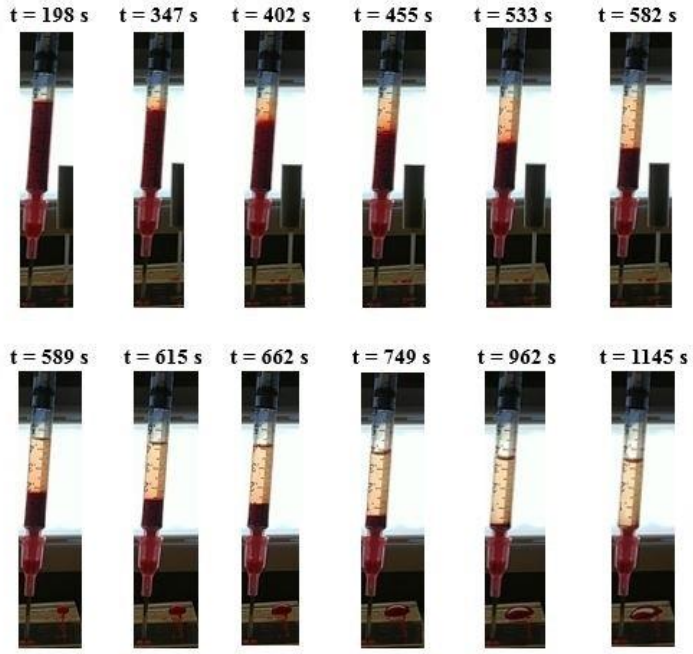

Figure 1-3 illustrated snapshot images captured at a specific time(t)

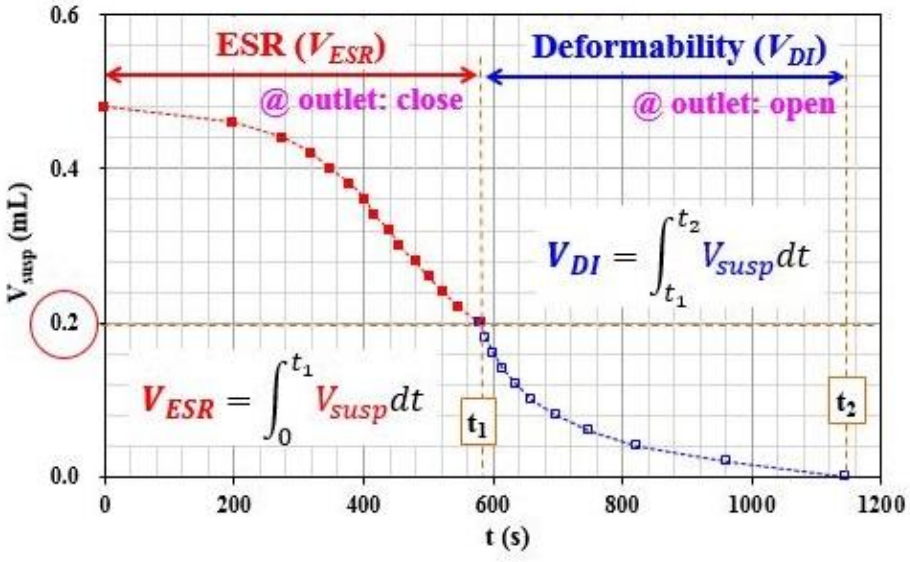

Figure 1-4 Quantification of ESR index (V_{ESR}) and RBC deformability index (V_{DI})

III. Results and discussion

A. Effect of several factors on two indices (V_{ESR}, and V_{DI})

It is required to evaluate the effect of several factors (i.e., air compression volume, pillar channel length, and hematocrit) on the two indices (i.e., V_{ESR}, and V_{DI}). Instead of autologous plasma, a specific concentration of dextran solution (i.e., 15mg/mL) as base solution was employed for reducing the elapsed time of ESR test.

First, the effect of air compression on the V_{ESR} was evaluated quantitatively by varying air compression volume (V_{comp}) (V_{comp}=0, and 0.4mL). Blood (Hct=30%) was prepared by adding normal RBCs into the specific dextran solution. As shown in **Fig. 2-1(a)**, temporal variations of V_{susp} were obtained by varying V_{comp}. ESR index (i.e., V_{ESR}) was calculated from the temporal variations of V_{SUSP}. As shown in **Figure 2-1(b)**, variation of the V_{ESR} was obtained with respect to V_{comp}. From the result, the air compression did not contribute to varying the ESR index significantly.

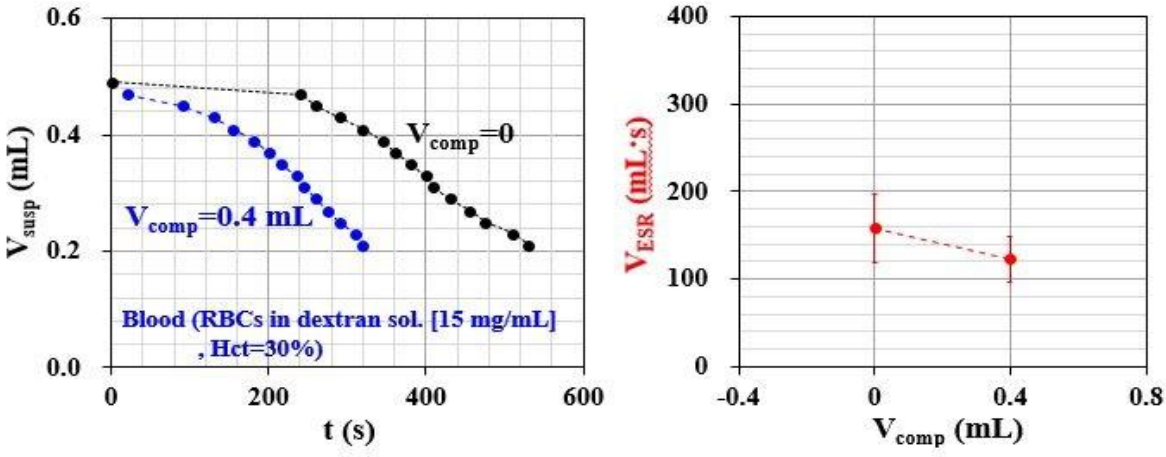

(a) (b)

Figure 2-1 The effect of air compression on the V_{ESR}. (a) Temporal variations of Vsusp with respect to Vcomp=0, and 0.4 mL. (b) Variations of V_{ESR} with respect to Vcomp=0, and 0.4 mL.

Second, the effect of pillar channel length (L) on the V_{DI} was quantified by varying L=50, 150, and 250μm. Blood (Hct=30%) was prepared by adding normal RBCs into the specific dextran solution. **Figure 2-2(a)** showed temporal variations of V_{susp} with respect to L. According to the result, the shorter channel length, the elapsed time for V_{susp}=0 tended to decrease. Because fluidic resistance is proportional to channel length, the shorter length had higher value of flow rate at the same pressure drop. Thus, the pillar channel with L=50μm had the shorter elapsed time, when compared with longer lengths. **Figure 2-2(b)** showed variations of V_{DI} with respect to L. From the result, the channel length had an influence on V_{DI}. For consistent measurement of RBC deformability, the length of pillar channel was fixed as L=150μm through all experiments.

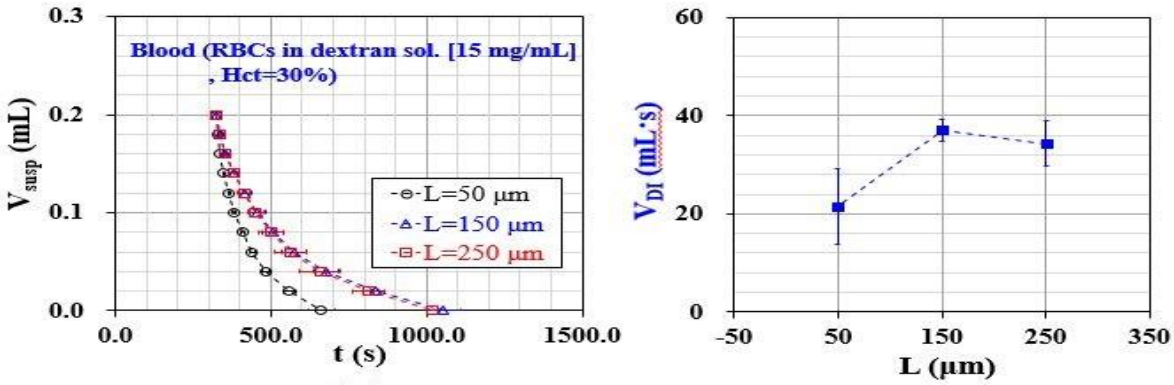

(a) (b)

Figure 2-2 The effect of pillar-channel length (L) on the $V_{DI.}$ (a) Variations of V_{susp} with respect to L=50, 150, and 250 μm. (b) Variations of V_{DI} with respect to $V_{DI.}$

Third, the effect of air compression on V_{ESR} and V_{DI} was quantified by varying air compression volume (V_{comp}) (Vcomp=0.2, 0.3, and 0.4mL). Blood (Hct=30%) was prepared by adding normal RBCs into the specific dextran solution. **Figure 2-3(a)** showed temporal variations of V_{susp} with respect to V_{comp}. The higher value of V_{comp}=0.4mL reduced the elapsed time of V_{susp}=0 largely, when compared with the others. With respect to V_{comp}=0.2mL, V_{susp} reduced to 0.08mL approximately after time elapse of 2500s. Thus, when calculating V_{DI} from the V_{susp}, t_2 was evaluated as the elapsed time of V_{susp} = 0.08mL. **Figure 2-3(b)** showed variations of V_{ESR} and V_{DI} with respect to V_{comp}=0.2, 0.3, and 0.4mL. From the results, V_{ESR} remained constant without respect to V_{comp}. In other words, the variation of air compression volume did not contribute to varying the ESR index. On the other hand, because the air compression volume caused to increase pressure developed in the ACS, it contributed to increasing blood flow rates. For this reason, V_{DI}

decreased largely by increasing V_{comp}. From the results, the V_{comp} contributed to varying V_{DI} significantly. But, it did not cause to change ESR index. In this study, V_{comp} was fixed as V_{comp}=0.4mL through all experiments.

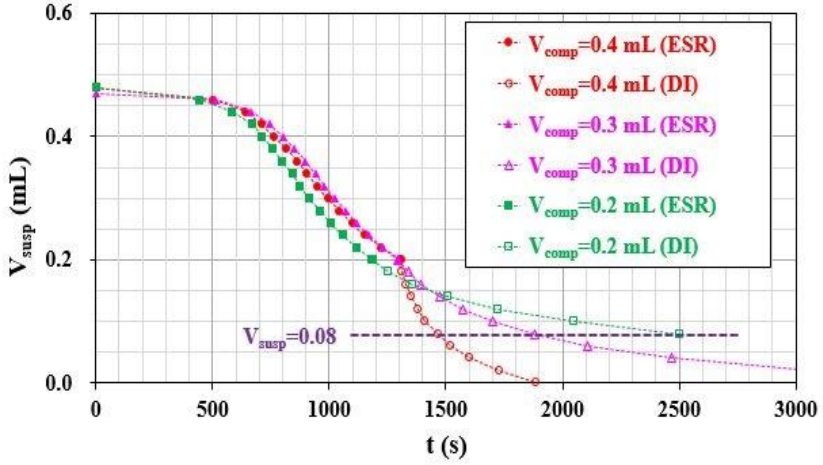

(a)

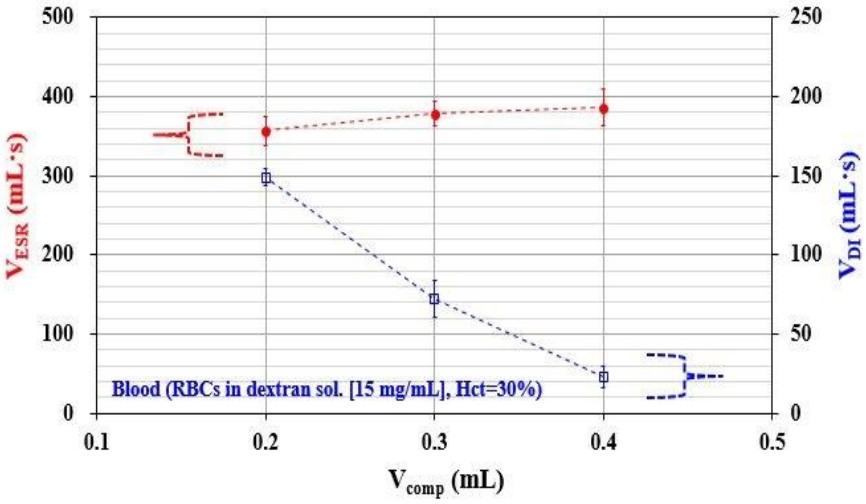

(b)

Figure 2-3 The effect of air compression (V_{comp}) on the V_{ESR} and V_{DI}. (a) Temporal variations of V_{susp} with respect to V_{comp}=0.2, 0.3, and 0.4 mL. (b) Variations of V_{ESR} and V_{DI} with respect to V_{comp}.

At last, the effect of hematocrit of V_{ESR} and V_{DI} was evaluated by varying the hematocrit level. Hematocrit of blood was adjusted to specific value (i.e., Hct=20%, 30%, 40%, and 50%) by adding normal RBCs into the specific dextran solution. Figure 2-4(a) showed temporal variations of V_{susp} with respect to Hct. From the result, at the close of outlet (i.e., ESR measurement) the elapsed time of V_{susp} decreased at lower hematocrit. At the open of outlet (i.e., DI measurement), the elapsed time of V_{susp} decreased at lower hematocrit similarly. Figure 2-4(b) represented variations of V_{ESR} and V_{DI} with respect to hematocrit. According to the results, hematocrit contributed to varying V_{ESR} and V_{DI}. In other words, the higher level of hematocrit increased the measurement time of ESR and RBC deformability largely. To decrease experiment time of ESR and DI, it is more appropriate to set lower value of hematocrit. In this study, the level of hematocrit was fixed as Hct=30% through all experiments.

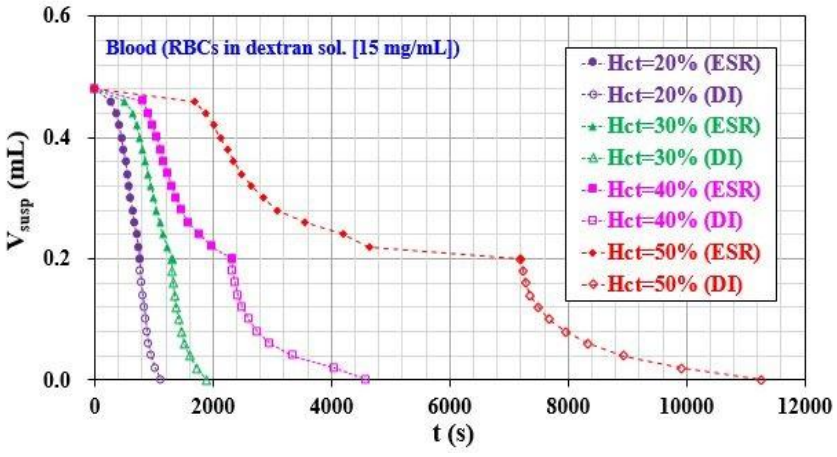

(a)

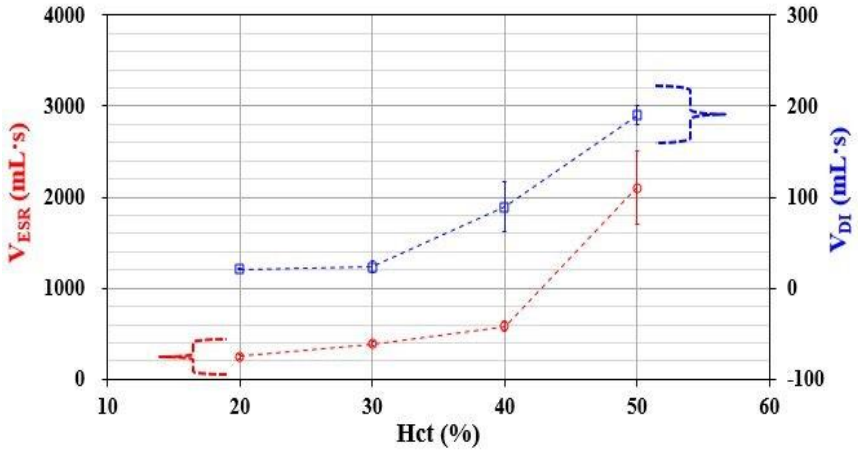

(b)

Figure 2-4 The effect of blood hematocrit of V_{ESR} and V_{DI}. (a) Temporal variations of V_{susp} with respect to Hct. (b) Variations of V_{ESR} and V_{DI} with respect to Hct.

B. Quantitative measurement of V_{ESR} and V_{DI} for dextran-included bloods

The proposed method was employed to measure V_{ESR} and V_{DI} simultaneously. To stimulate ESR of bloods, various concentrations of dextran solution (i.e., C_{dex}=5, 10, 15, 20, and 25mg/mL) were prepared. Control (i.e., C_{dex}=0) indicates plasma as base solution. Each blood (Hct=30%) was prepared by adding normal RBCs into a specific concentration of dextran solution.

Figure 3(a) showed temporal variations of V_{susp} with respect to C_{dex}. In addition, the inset represented variations of V_{susp} with respect to C_{dex}=15 and 20mg/mL. From the results, the dextran solution contributed to

decrease the elapsed time of ESR largely. But, it did not have an influence on the elapsed time of RBC deformability. As shown in **Fig. 3(b)**, variations of V_{ESR} and VDI were obtained by varying the concentration of dextran solution. From the results, The V_{ESR} decreased largely at higher concentration of dextran solution. Above C_{dex}=15mg/mL, the V_{ESR} remained constant. In other words, dextran solution caused to increase ESR index significantly. When compared with the previous results[33,45], the proposed method gave consistent variations with respect to the concentration of dextran solution. On the other hand, V_{DI} remained constant without respect to C_{dex}. According to the previous measurement of viscoelasticity[59], blood viscoelasticity remained constant with respect to the concentration of dextran solution. By referring to the fact that blood viscoelasticity is strongly related with RBC deformability, the previous result indicated that RBC deformability remained constant within the specific concentration of dextran solution. Thus, the proposed method gave consistent results when compared with the previous result. From the experimental results, it was found that the proposed method has the ability to measure ESR with consistency.

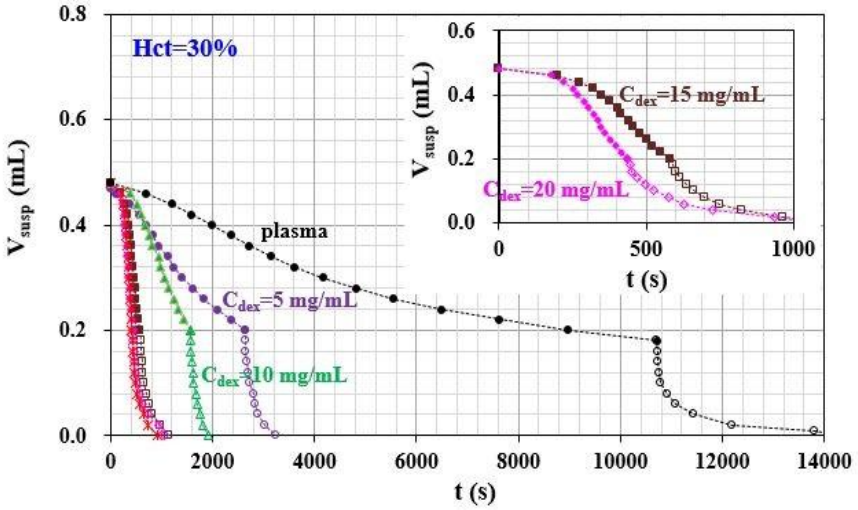

(a)

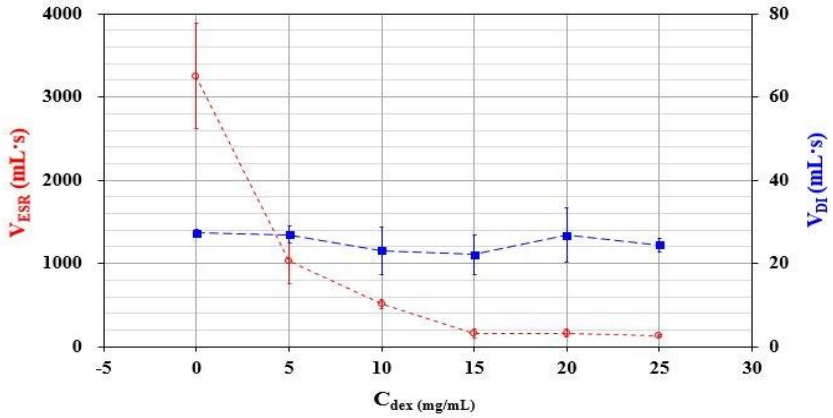

(b)

Figure 3 Quantitative evaluations of V_{ESR} and V_{DI} for dextran-included blood. (a) Temporal variations of V_{susp} with respect to C_{dex}. Insets represented temporal variations of V_{susp} with respect to C_{dex}=15 and 20mg/mL. (b) Variations of V_{ESR} and V_{DI} with respect to C_{dex}.

C. Variations of V_{ESR} and V_{DI} for heterogeneous bloods

As a performance demonstration, the proposed method was employed to detect heterogeneous bloods. The heterogeneous blood was prepared by mixing normal blood with hardened blood partially.

First, to decrease deformability of normal RBCs, normal RBCs were dipped them into specific concentration of glutaraldehyde (GA) solution (C_{GA}) (C_{GA}=2, 4, 6, and 8μL/mL). The hardened blood (Hct=30%) was prepared by adding hardened RBCs into 1x PBS solution. As controls, normal RBCs were added into plasma and PBS solution, respectively. Because the hardened blood did not include plasma proteins, it did not contribute to inducing ESR. As show in **Fig. 4(a)**, at the open of outlet (i.e., deformability measurement), the variations of V_{SUSP} were obtained by varying C_{GA}. From the results, the elapsed time of ESR tended to decrease at higher concentration of GA solution. With respect to C_{GA}=8μL/mL, V_{susp} remained constant over time. In other words, the hardened blood with C_{GA}=8μL/mL did not pass through the micropillar channels at all.

From the experimental results, hardened blood was prepared by adding RBCs fixed by GA solution (C_{GA}=8μL/mL) into PBS solution (i.e., V_{GA}). In addition, to reduce the elapsed time of experiments, normal blood was prepared by adding normal RBCs into specific dextran solution (15mg/mL) rather than plasma. Using two bloods (i.e., normal blood and hardened blood), heterogeneous blood was then prepared by adding hardened blood into normal blood partially. Here, the mixing ratio (ϕ) was defined as

$\phi = \frac{V_{GA}}{V_{dex} + V_{GA}}$. As shown in **Fig. 4(b)**, temporal variations of V_{susp} were obtained by varying ϕ=0, 5%, and 10%. Here, ϕ=0 did not include hardened bloods. According to the result, the elapsed time of ESR increased largely at ϕ=10%. But, ϕ=0 and ϕ=5% did not show difference in ESR. As shown in **Fig. 4(c)**, variations of V_{ESR} and V_{DI} were obtained by varying ϕ. Less than ϕ=10%, V_{ESR} did not show significant difference with respect to ϕ. Similarly, V_{DI} did show significant difference from ϕ=10%. In other words, two indices V_{ESR} (ESR) and V_{DI} (RBC deformability) were varied significantly above ϕ=10%.

From the results, it leads to the conclusion that the proposed method has the ability to detect heterogeneous blood with at least 10% hardened blood. In addition, two indices (i.e., V_{ESR} and V_{DI}) were employed to quantify the degree of ESR and RBC deformability effectively.

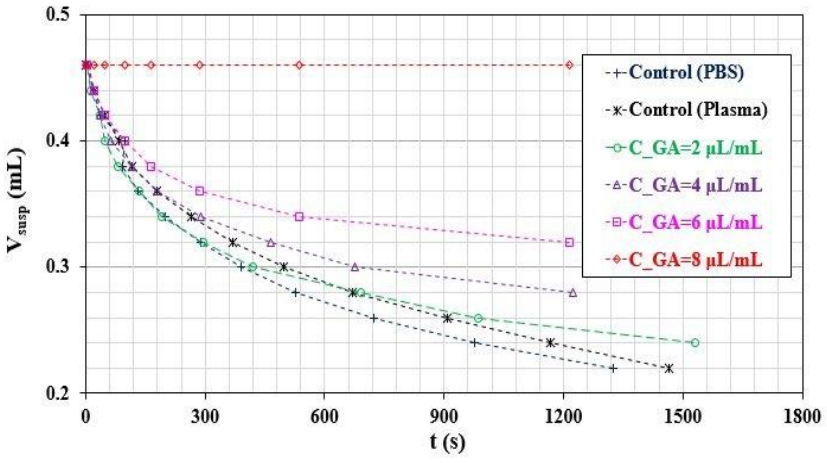

(a)

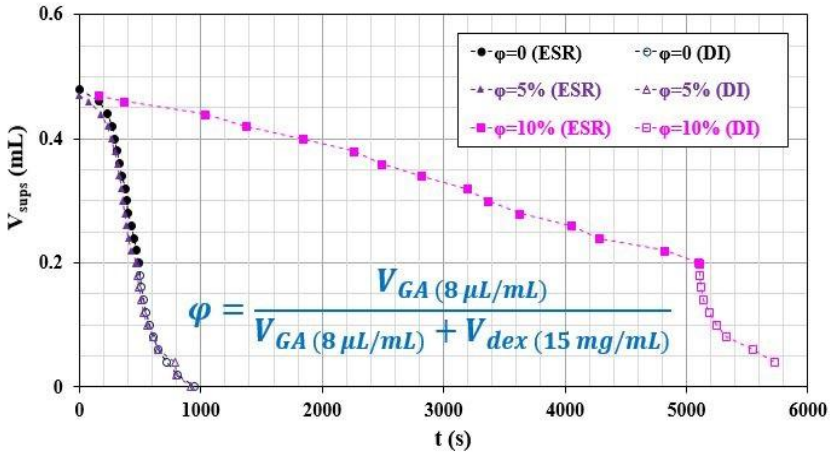

(b)

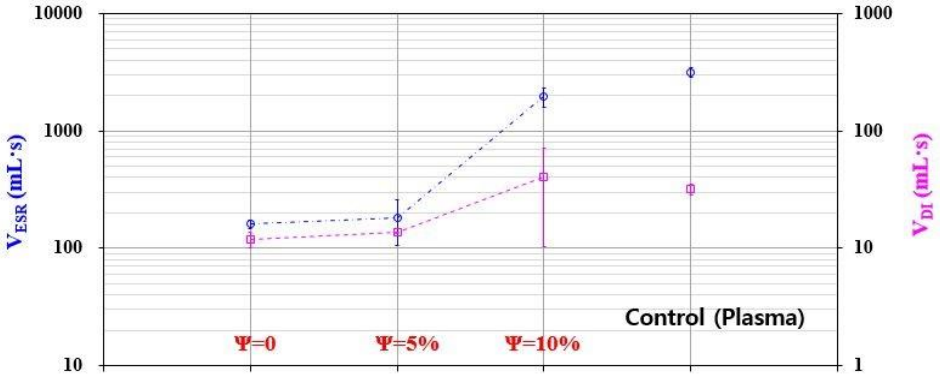

(c)

Figure 4 Simultaneous measurement of V_{ESR} and V_{DI} for heterogeneous bloods. (a) Variations of V_{susp} with respect to specific concentration of glutaraldehyde (GA) solution (C_{GA}=2, 4, 6, and 8μL/mL). (b) Temporal variations of V_{susp} with respect to mixing ratio (ϕ=0, 5, and 10%). (c) Variations of V_{ESR} and V_{DI} with respect to ϕ.

IV. Conclusion

In this study, a simple method for sequential measurement of ESR and RBC deformability was demonstrated by quantifying the volume of suspended blood in the ACS. To demonstrate the proposed method, a microfluidic device was composed of multiple micropillar channels, inlet, and outlet. The ACS was composed of a disposable syringe and a fixture. The ACS was partially filled with air (~0.4mL) and blood (~0.6mL) sequentially. By closing the outlet with a stopper, the needle of the ACS was tightly fitted into the inlet. Using the fixture, the volume of air compression was adjusted to 0.4mL (i.e., V_{comp}=0.4mL). Using smartphone camera, snapshot images were sequentially captured to monitor the volume of suspended blood inside the ACS (i.e., V_{susp}). At the close of the outlet, the variations of V_{susp} were obtained until V_{susp} decreased to V_{susp}=0.2mL. ESR index (i.e., V_{ESR}) was obtained by quantifying the variations of V_{susp} over time. At the open of the outlet, the variations of V_{susp} were obtained until V_{susp} decreased to V_{susp}=0. RBC deformability index (V_{DI}) was obtained by analyzing variations of V_{susp} over time.

From the experimental demonstrations, the following results were obtained as,

■ The effect of pillar channel length (L) on the V_{DI} was quantified by varying L=50, 150, and 250μm. At the close of the outlet (i.e., RBC deformability), the shorter length of micropillar (L=50μm) reduced the

elapsed time for decreasing V_{susp} from V_{susp}=0.2mL to V_{susp}=0. The V_{DI} did not show significant difference with respect to L=150 and 250μm. From the results, the length of pillar channel was fixed as L=150μm through all experiments.

■ The effect of air compression on V_{ESR} and V_{DI} was quantified by varying air compression volume (V_{comp}) (V_{comp}=0.2, 0.3, and 0.4mL). The V_{comp} contributed to varying V_{DI} significantly. But, it did not cause to alter ESR index. Thus, the volume of air compression (V_{comp}) was fixed as V_{comp}=0.4mL through all experiments.

■ The effect of hematocrit of V_{ESR} and V_{DI} was evaluated by varying the hematocrit level (Hct) (Hct =20%, 30%, 40%, and 50). The higher level of hematocrit increased measurement time of ESR and RBC deformability significantly.

■ The proposed method was employed to measure V_{ESR} and V_{DI} for dextran-included bloods. The dextran solution contributed to decrease the elapsed time of ESR largely. But, it did not have an influence on the elapsed time of RBC deformability. When compared with the previous studies, the proposed method gave consistent results.

■ As a performance demonstration, the proposed method was employed to detect heterogeneous bloods. The heterogeneous blood was prepared

by mixing normal blood with hardened blood partially. Less than mixing ratio of ϕ=10%, V_{ESR} did not show significant difference with respect to ϕ. Similarly, V_{DI} did show significant difference from ϕ=10%. In other words, two indices V_{ESR} (ESR) and V_{DI} (RBC deformability) were varied significantly above ϕ=10%.

From the results, it leads to the conclusion that the proposed method has the ability to detect heterogeneous blood with at least 10% hardened blood. In addition, two indices (i.e., V_{ESR} and V_{DI}) were employed to quantify ESR and RBC deformability effectively. However, the proposed method did not apply for clinical tests. As a future work, it will be required to verify the performance of the proposed methods for clinical samples such as cardiovascular diseases or malaria-infected bloods. Furthermore, through various experimental results, it will be required to understand distinctive trends of ESR and RBC deformability depending on various diseases.

References

(1) E. J. Benjamin, P. Muntner, A. Alonso, M. S. Bittencourt, C. W. Callaway, A. P. Carson, A. M. Chamberlain, A. R. Chang, S. Cheng, S. R. Das, et al., 2019, "Heart disease and stroke statistics—2019 update", Circulation, 139, pp. e56-e528.

(2) Y. J. Kang and S.-J. Lee, 2018, "In vitro and ex vivo measurement of the biophysical properties of blood using microfluidic platforms and animal models", Analyst, 143, pp. 2723-2749.

(3) A. H. B. Wu, 2005, "Markers for early detection of cardiac diseases", Scand. J. Clin. Lab. Invest. Suppl., 240, pp. 112-121.

(4) J. Yayan, 2012, "Erythrocyte sedimentation rate as a marker for coronary heart disease", Vasc. Health Risk Manag., 8, pp. 219-223.

(5) J. Danesh, R. Collins, R. Peto, and G. D. O. Lowe, 2000, "Haematocrit, viscosity, erythrocyte sedimentation rate: meta-analyses of prospective studies of coronary heart disease", Eur. Heart J. , 21, pp. 515-520.

(6) A. S. Popel and P. C. Johnson, 2005, "Microcirculation and hemorheology", Annu. Rev. Fluid Mech., 37, pp. 43-69.

(7) B. Sebastian and P. S. Dittrich, 2018, "Microfluidics to mimic blood flow in health and disease", Annu. Rev. Fluid Mech., 50, pp. 483-504.

(8) Y. J. Kang, 2018, "A disposable blood-on-a-chip for simultaneous measurement of multiple biophysical properties", Micromachines, 9, pp. 475.

(9) Y. J. Kang, Y.-R. Ha, and S.-J. Lee, 2016, "High-Throughput and Label-Free Blood-on-a-Chip for Malaria Diagnosis", Anal. Chem., 88, pp. 2912-2922.

(10) Y. Zheng, J. Nguyen, Y. Wei, and Y. Sun, 2013, "Recent advances in microfluidic techniques for single-cell biophysical characterization", Lab Chip, 13, pp. 2464-2483.

(11) O. K. Baskurt, D. Gelmont, and H. J. Meiselman, 1998, "Red blood cell deformability in sepsis", Am. J. Respir. Crit. Care Med., 157, pp. 421-427.

(12) S. S. Shevkoplyas, T. Yoshida, S. C. Gifford, and M. W. Bitensky, 2006, "Direct measurement of the impact of impaired erythrocyte deformability on microvascular network perfusion in a microfluidic device", Lab Chip, 6, pp. 914-920.

(13) T. Herricks, M. Antia, and P. K. Rathod, 2009, "Deformability limits of Plasmodium falciparum-infected red blood cells", Cell Microbiol., 11, pp. 1340-1353.

(14) J. Zhang, P. C. Johnson, and A. S. Popel, 2009, "Effects of erythrocyte deformability and aggregation on the cell free layer and apparent viscosity of microscopic blood flows", Microvasc. Res., 77, pp. 265-272.

(15) M. R. Amaiden, N. E. Monesterolo, V. S. Santander, A. N. Campetelli, C. A. Arce, S. I. Hope, M. S. Vatta, and C. H. Casale, 2012, "Involvement of membrane tubulin in erythrocyte deformability and blood pressure", J. Hypertens., 30, pp. 1414-1422.

(16) J. P. Beech, S. H. Holm, K. Adolfssona, and J. O. Tegenfeldt, 2012, "sorting cells by size, shape and deformability", Lab Chip, 12, pp. 1048-1051.

(17) Q. Guo, S. Park, and H. Ma, 2012, "Microfluidic micropipette aspiration for measuring the deformability of single cells", Lab Chip, 12, pp. 2687-2695.

(18) S. Huang, A. Undisz, M. Diez-Silva, H. Bow, M. Dao, and J. Han, 2013, "Dynamic deformability of Plasmodium falciparum-infected erythrocytes exposed to artesunate in vitro", Integr. Biol., 5, pp. 414-422.

(19) J. C. A. Cluitmans, V. Chokkalingam, A. M. Janssen, R. Brock, W. T. S.Huck, and GielJ.C.G.M.Bosman, 2014, "Alterations in red blood cell deformability during storage: a microfluidic approach", Biomed Res. Int., 2014, pp. 764268.

(20) R. Agrawal, T. Smart, J. Nobre-Cardoso, C. Richards, R. Bhatnagar, A. Tufail, D. Shima, P. H. Jones, and C. Pavesio, 2016, "Assessment of red blood cell deformability in type 2 diabetes mellitus and diabetic retinopathy by dual optical tweezers stretching technique", Sci. Rep., 6, pp. 15873.

(21) Q. Guo, S. P. Duffy, K. Matthews, X. Deng, A. T. Santoso, E. Islamzada, and H. Ma, 2016, "Deformability based sorting of red blood cells improves diagnostic sensitivity for malaria caused by Plasmodium falciparum", Lab Chip, 16, pp. 645-654.

(22) H. Park, S. Lee, M. Ji, K. Kim, Y. Son, S. Jang, and Y. Park, 2016, "Measuring cell surface area and deformability of individual human red blood cells over blood storage using quantitative phase imaging", Sci. Rep., 6, pp. 34257.

(23) N. F. Zeng, J. E. Mancuso, A. M. Zivkovic, J. T. Smilowitz, and W. D. Ristenpart, 2016, "Red blood cells from individuals with abdominal obesity or metabolic abnormalities exhibit less deformability upon entering a constriction", PLoS One, 11, pp. e0156070.

(24) L. V. Boas, V. Faustino, R. Lima, J. M. Miranda, G. Minas, C. S. V. Fernandes, and S. O. Catarino, 2018, "Assessment of the deformability and velocity of healthy and artificially impaired red blood cells in narrow polydimethylsiloxane (PDMS) microchannels", Micromachines, 9, pp. 384.

(25) Y. J. Kang, 2018, "RBC deformability measurement based on variations of pressure in multiple micropillar channels during blood delivery using a disposable air-compressed pump", Anal. Methods, 10, pp. 4549-4561.

(26) Y. J. Kang, 2017, "Simultaneous measurement of erythrocyte deformability and blood viscoelasticity using micropillars and co-flowing streams under pulsatile blood flows", Biomicrofluidics, 11, pp. 014102.

(27) S. H. Song, J. H. Kim, J. H. Lee, Y.-M. Yun, D.-H. Choi, and H. Y. Kim, 2017, "Elevated blood viscosity is associated with cerebral small vessel disease in patients with acute ischemic stroke", BMC Neurol., 17, pp. 20.

(28) G. A. M. Pop, L. L. A. Sisschops, B. Iliev, P. C. Struijk, J. G. v. d. Heven,

and C. W. E. Hoedemaekers, 2013, "On-line blood viscosity monitoring in vivo with a central venous catheter using electrical impedance technique", Biosens. Bioelectron., 41, pp. 595-601.

(29) H. Kim, Y. I. Cho, D.-H. Lee, C.-M. Park, H.-W. Moon, M. Hur, J. Q. Kim, and Y.-M. Yun, 2013, "Analycal performance evaluation of the scanning tube viscometer for measurement of whole blood viscosity", Clin. Biochem., 46, pp. 139-142.

(30) S. Shin, J. H. Jang, M. S. Park, Y. H. Ku, and J. S. Suh, 2005, "A noble RBC aggregometer with vibration-induced disaggregation mechanism", Korea-Aust. Rheol. J., 17, pp. 9-13.

(31) K. Lee, M. Kinnunen, M. D. Khokhlova, E. V. Lyubin, A. V. Priezzhev, I. Meglinski, and A. A. Fedyanin, 2016, "Optical tweezers study of red blood cell aggregation and disaggregation in plasma and protein solutions", J. Biomed. Opt., 21, pp. 035001.

(32) W. H. Reinhart, N. Z. Piety, and S. S. Shevkoplyas, 2017, "Influence of red blood cell aggregation on perfusion of an artificial microvascular network", Microcirculation, 24, pp. e12317.

(33) Y. J. Kang and B. J. Kim, 2018, "Multiple and periodic measurement of RBC aggregation and ESR in parallel microfluidic channels under on-off blood flow control", Micromachines, 9, pp. 318.

(34) E. Yeom and S.-J. Lee, 2015, "Microfluidic-based speckle analysis for sensitive measurement of erythrocyte aggregation: A comparison of four methods for detection of elevated erythrocyte aggregation in diabetic rat blood", Biomicrofluidics, 9, pp. 024110.

(35) J. M. Sherwood, J. Dusting, E. Kaliviotis, and S. Balabani, 2012, "The effect of red blood cell aggregation on velocity and cell-depleted layer characteristics of blood in a bifurcating microchannel", Biomicrofluidics, 6, pp. 024119.

(36) H.-J. Lim, J.-H. Nam, B.-K. Lee, J.-S. Suh, and S. Shin, 2011, "Alteration of red blood cell aggregation during blood storage", Korea-Aust. Rheol. J.,

23, pp. 67-70.

(37) C. B. Ahn, Y. J. Kang, M. G. Kim, S. Yang, C. H. Lim, H. S. Son, J. S. Kim, S. Y. Lee, K. H. Son, and K. Sun, 2016, "The effect of pulsatile versus nonpulsatile blood flow on viscoelasticity and red blood cell aggregation in extracorporeal circulation", Korean J. Thorac. Cardiovasc. Surg., 49, pp. 145-150.

(38) K. Bochen, A. Krasowska, S. Milaniuk, M. Kulczyńska, A. Prystupa, and G. Dzida, 2011, "Erythrocyte sedimentation rate-an old marker with new applications", JPCCR, 5, pp. 50-55.

(39) T. L. Fabry, 1987, "Mechanism of erythrocyte aggregation and sedimentation", Blood, 70, pp. 1572-1576.

(40) K. Odashiro, K. Saito, T. Arita, T. Maruyama, T. Fujino, and K. Akashi, 2015, "Impaired deformability of circulating erythrocytes obtained from nondiabetic hypertensive patients: investigation by a nickel mesh filtration technique", Clinical Hypertension, 21, pp. 17.

(41) W. Groner, N. Mohandas, and M. Bessis, 1980, "New optical technique for measuring erythrocyte deformability with the ektacytometer", Clin. Chem., 26(10), pp. 1435-1442.

(42) K. Cha, E. F. Brown, and D. W. Wilmore, 1994, "A new bioelectrical impedance method for measurement of the erythrocyte sedimentation rate", Physiol. Meas. , 15, pp. 499-508.

(43) T.-X. Zhao and B. Jacobson, 1997, "Quantitative correlations among fibrinogen concentration, sedimentation rate and electrical impedance of blood", Med. Biol. Eng. Compt., 35, pp. 181-185.

(44) A. Zhbanov and S. Yang, 2015, "Effects of aggregation on blood sedimentation and conductivity", PLoS One, 10, pp. e0129337.

(45) Y. J. Kang, Y.-R. Ha, and S.-J. Lee, 2014, "Microfluidic-based measurement of erythrocyte sedimentation rate for biophysical assessment of blood in an in vivo malaria-infected mouse", Biomicrofluidics, 8, pp.

044114.

(46) Y. J. Kang, 2018, "Microfluidic-based measurement of RBC aggregation and the ESR using a driving syringe system", Anal. Methods, 10, pp. 1805-1816.

(47) Y. J. Kang, 2017, "Microfluidic-based measurement method of red blood cell aggregation under hematocrit variations", Sensors, 17, pp. 2037.

(48) A. Chaturvedi, S. K. Nagaraj, S. S. Gorthi, and C. S. Seelamantula, 2017, "An efficient microscale technique for determining the erythrocyte sedimentation rate", SLAS Technology, 22(5), pp. 565-572.

(49) Z. Isiksacan, O. Erel, and C. Elbuken, 2016, "A portable microfluidic system for rapid measurement of the erythrocyte sedimentation rate", Lab Chip, 16, pp. 4682-4690.

(50) J. P. Shelby, J. White, K. Ganesan, P. K. Rathod, and D. T. Chiu, 2003, "A microfluidic model for single-cell capillary obstruction by Plasmodium falciparuminfected erythrocytes", Proc. Natl. Acad. Sci. U. S. A., 100, pp. 14618-14522.

(51) Y.-C. Chen, G.-Y. Chen, Y.-C. Lin, and G.-J. Wang, 2010, "A lab-on-a-chip capillary network for red blood cell hydrodynamics", Microfluid. Nanofluid., 9, pp. 585-591.

(52) P. Preira, V. Grandne, J.-M. Forel, S. Gabriele, M. Camaraa, and O. Theodoly, 2013, "Passive circulating cell sorting by deformability using a microfluidic gradual filter", Lab Chip, 13, pp. 161-170.

(53) Y. N. Luo, and others. 2014, "A constriction channel based microfluidic system enabling continuous characterization of cellular instantaneous Young's modulus", Sens. Actuator B-Chem., 202, pp. 1183-1189.

(54) Q. Guo, S. J. Reiling, P. Rohrbach, and H. Ma, 2012, "Microfluidic biomechanical assay for red blood cells parasitized by Plasmodium falciparum", Lab Chip, 12, pp. 1143-1150.

(55) M. J. Rosenbluth, W. A. Lam, and D. A. Fletcher, 2008, "Analyzing cell mechanics in hematologic diseases with microfluidic biophysical flow cytometry", Lab Chip, 8, pp. 1062-1070.

(56) J. R. Lange, C. Metzner, S. Richter, W. Schneider, M. Spermann, T. Kolb, G. Whyte, and B. Fabry, 2017, "Unbiased high-precision cell mechanical measurements with microconstrictions", Biophys. J., 112, pp. 1472-1480.

(57) H. Bow, I. V. Pivkin, M. Diez-Silva, S. J. Goldfless, M. Dao, J. C. Niles, S. Sureshb, and J. Han, 2011, "A microfabricated deformability-based flow cytometer with application to malaria", Lab Chip, 11, pp. 1065-1073.

(58) Y. J. Kang, Y.-R. Ha, and S.-J. Lee, 2016, "Deformability measurement of red blood cells using a microfluidic channel array and an air cavity in a driving syringe with high throughput and precise detection of subpopulations", Analyst, 141, pp. 319-330.

(59) E. Du, S. Ha, M. Diez-Silva, M. Dao, S. Suresh, and A. P. Chandrakasan, 2013, "Electric impedance microflow cytometry for characterization of cell disease states", Lab Chip, 13, pp. 3903-3909.

(60) Y. Zheng, E. S. Baghini, A. Azad, C. Wang, and Y. Sun, 2012, "High-throughput biophysical measurement of humna red blood cells", Lab Chip, 12, pp. 2560-2567.

(61) Y. J. Kang, 2016, "Continuous and simultaneous measurement of the biophysical properties of blood in a microfluidic environment", Analyst, 141, pp. 6583-6597.

Supplementary Materials

■ Fig. S1

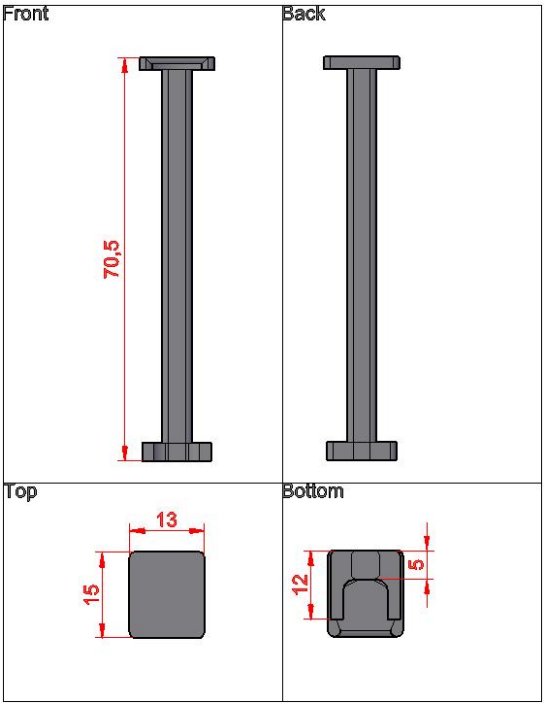

■ Fig. S2